Assessing the thermal environment of major cities in Greece

M. Stathopoulou, C. Cartalis and A. Andritsos
University of Athens, Greece

ABSTRACT

Satellite images in the thermal infrared can be used for assessing the thermal urban environment as well as for defining heat islands in urban areas. In this paper, the thermal environment of major cities in Greece (Athens, Thessaloniki, Patra, Volos and Heraklion) is examined by using satellite images provided by the Landsat Enhanced Thematic Mapper (ETM+) sensor on board Landsat 7 platform corresponding to daytime and warm period, when the surface urban heat island (UHI) phenomenon is best observed. The spatial structure of the thermal urban environment is analyzed in each case study and the "hottest" surfaces within the urban settings are identified and related to the urban surface characteristics and land use. For the needs of the study, the Corine land cover (CLC) database for Greece is used, in an effort to define more effectively the link between emissivities, surface temperatures and urban surface characteristics. Results are examined with respect to the specific city characteristics and are used for supporting urban – land use – planning.

1. INTRODUCTION

Urban heat island (UHI) phenomenon describes the excess warmth of the urban atmosphere compared to the non-urbanized rural surroundings. The main reasons of this phenomenon include construction materials of high heat capacity and low solar reflectivity such as asphalt and concrete, reduced turbulent heat transfer due to street canyons geometry, reduced latent heat loss by evaporation due to the replacement of the natural green surfaces with dry surfaces and increased anthropogenic heat emissions into the urban atmosphere. The magnitude of the UHI is reflected by the temperature differences between urban and rural sites and depends on the size, population and industrial development of a city, topography, physical layout, regional climate and meteorological conditions (Oke et al., 1987).

Voogt and Oke (2003) review the use of thermal remote sensing for the study of urban climates with respect to the UHI effect and describe the distinction between the atmospheric UHI and the surface UHI. Atmospheric UHI is usually detected by ground-based air temperature measurements taken from standard meteorological stations, whereas surface UHI is observed from thermal remote sensors which record the upwelling thermal radiance emitted by the surface area that lies within the instantaneous field of view (IFOV) of the sensor. In contrast to atmospheric UHIs that are best expressed under calm and clear conditions at night, surface UHIs are usually studied by using satellite thermal remote sensing data of high spatial resolution (~ 100 m) acquired at daytime when heat island intensities are greatest (Roth et al., 1989).

Many surface UHI studies have been conducted using thermal remote sensing from satellites (Aniello et al., 1995; Streutker, 2002; Dousset and Gourmelon, 2003). These studies give a spatially continuous view of the surface UHI over large urban areas than is feasible using data from meteorological station networks. In addition, remote sensing can effectively depict the thermal environment of urban areas on a repeated basis. Thus, spatial coverage and temporal repetition are the main advantages of using satellite thermal remote sensing technique in

the study of the urban climates.

For the region of Greece, a recent study using thermal remote sensing data of medium spatial resolution showed that the surface UHI intensity at night can reach up to 8°C for the cities of Thessaloniki and Heraklion and up to 7°C for the cities of Patra and Volos (Stathopoulou et al., 2004). From another study using air temperature measurements (Santamouris et al., 2001), it was found that during the summer period, daytime UHI intensity of Athens is close to 10°C for the central Athens area, whereas the night-time UHI intensity can rise up to 5°C.

This study presents a methodology for estimating the surface UHI intensity of urban areas by using satellite images in combination with land cover information provided by the Corine land cover database for Greece. The method is applied to the major cities of Greece: Athens, Thessaloniki, Volos, Patra and Heraklion in order to study their thermal environment.

2. METHODOLOGY

The methodology for mapping and estimating surface UHI intensities involves:

- Landsat ETM+ processing so as to obtain at-sensor brightness temperatures.
- CLC data processing for the spatial definition of the urban, suburban, mixed and rural sites of the city, which allows further the more spatially accurate determination of their respective surface emissivities.
- Surface temperature mapping.
- Surface UHI intensity estimation based on the mean surface temperature differences between urban and rural sites of the city.

2.1 Landsat ETM+ processing

Landsat 7 ETM+ thermal images are used in order to map the thermal urban environment of the cities of Athens (37° 58′N, 23° 46′E), Thessaloniki (40° 38′N, 22° 58′E), Patra (38° 14′N, 21° 47′E), Volos (39° 24′N, 22° 59′E) and Heraklion (35° 20′N, 25° 12′E). ETM+ thermal band 6 (10.4 - 12.5 μm) has a spatial resolution of 60 m at nadir, which is considered to be suitable for capturing the complex intra-urban temperature differences allowing thus, an effective and detailed analysis of the urban climate. Table 1 lists the acquisition date and time of the Landsat ETM+ images recorded over the selected cities. All images correspond to highly clear atmospheric conditions and warm season. They were acquired through the US Geological Survey (USGS) Earth Resource Observation Systems Data Center and are the best images available, given that the local time of the satellite overpasses over the region of Greece is near solar noon time (12:00 am).

Thermal band image data calibration is performed in a two-step process as proposed by the Landsat Project Science Office (2002): a) conversion of the digital number (DN) values of band 6 into spectral radiance L ($Wm^{-2}sr^{-1}\mu m^{-1}$) using the following equation:

$$L = 0.0370588 \times DN + 3.2 \quad (1)$$

and then b) conversion of the spectral radiance L to at-sensor brightness temperature BT in Kelvin. The conversion formula is given by:

$$BT = K_2 / \{\ln [(K_1/L) + 1]\} \quad (2)$$

where:

BT: at-sensor brightness temperature in K
K_2: calibration constant (1282.71 K)
K_1: calibration constant (666.09 $Wm^{-2}sr^{-1}\mu m^{-1}$)
L: spectral radiance at-sensor ($Wm^{-2}sr^{-1}\mu m^{-1}$).

2.2 Corine land cover data processing

Corine land cover (CLC) is a geographic land cover/land use database for a pan-European region. It describes land cover using a nomenclature of 44 classes organized in 3 levels of detail at the scale of 1: 100 000 (European Commission, 1994). The CLC database for Greece in vector format is utilized in this study in an effort to link more effectively land cover and surface emissivity.

From the original CLC layer a new polygon layer is reproduced that contains the 5 land cover types (classes) of: urban/densely built area, suburban area, mixed urban area, rural area and sea. The new class assignment is clearly

Table 1: Landsat ETM+ images used in this study.

City	Date (d/m/y)	Time (UTC)
Athens	20/05/2000	08:57
Thessaloniki	30/05/2001	09:00
Volos	24/08/2000	08:56
Patra	28/06/2000	09:02
Heraklion	09/07/2000	08:45

shown in Table 2. The aggregated land cover layer aims at the spatial discrimination between the different urban land covers that are related to the UHI phenomenon and also favours the spatially accurate assignment of the surface emissivity that corresponds to these urban land covers. Table 3 shows the emissivity values for the different land covers used in this study.

2.3 Surface temperature retrieval

Brightness temperature derived from Equation (2) is the temperature that a blackbody would obtain in order to produce the same radiance at the same wavelength (λ =11.5 μm). Additional correction for spectral emissivity is required for the non-uniform emissivity of the land surface. Therefore, each of the land cover classes is assigned an emissivity value from Table 3 and the emissivity corrected surface temperature T_s is computed as follows:

$$T_s = BT/\{1 + [(\lambda BT/\rho)\times \ln\varepsilon]\} \quad (3)$$

where:

T_s: surface temperature (K)
BT: at-sensor brightness temperature (K)
λ: wavelength of emitted radiance (11.5 μm)
ρ: $(h\times c/\sigma) = 1.438\times 10^{-2}$ m K
ε: spectral surface emissivity.

Table 2: Original Corine and grouped land cover classes.

Code	CLC classes	New class assignment
111	Continuous urban fabric	Urban/densely built
112	Discontinuous urban fabric	Suburban/medium built
121	Industrial or commercial units	Mixed urban area
122	Road & rail networks	Mixed urban area
123	Port areas	Mixed urban area
124	Airports	Mixed urban area
131	Mineral extraction sites	Mixed urban area
132	Dump sites	Mixed urban area
133	Construction sites	Mixed urban area
141	Green urban areas	Suburban/medium built
142	Sport & leisure facilities	Mixed urban area
211	Non-irrigated arable land	Rural
221	Vineyards	Rural
222	Fruit trees & berry plantations	Rural
223	Olive trees	Rural
241	Annual crops associated with...	Rural
242	Complex cultivation patterns	Rural
243	Land principally occupied by...	Rural
244	Agro-forestry areas	Rural
312	Coniferous forests	Rural
313	Mixed forests	Rural
321	Natural grassland	Rural
322	Moors & heathland	Rural
323	Sclerophyllous vegetation	Rural
324	Transitional woodland shrub	Rural
331	Beaches, dunes & sand plains	Rural
332	Bare rock	Rural
333	Sparsely vegetated areas	Rural
334	Burnt areas	Rural
523	Sea and oceans	Sea

Table 3: Emissivity values by land cover type.

Land cover type	Emissivity
Urban/densely built	0.946
Suburban area	0.964
Mixed urban are	0.950
Rural area	0.980
Sea	0.990

Taken that this study is interested in relative temperature differences between urban and rural sites, the error due to the atmospheric effects is not corrected. Since the UHI effect is studied in a spatial extent of a few kilometers around the city center (local scale), it is reasonable to assume the homogeneity of the atmosphere over the urban area. The error in the land brightness temperature subject to the influence of the atmospheric conditions is relatively uniform across the image and it is adjusted in case that temperature differences are examined.

2.4 Estimation of the surface UHI intensity

The surface UHI estimation is completed by combining the surface temperature data (in raster format) with the reproduced land cover data (in vector format). In particular, the land cover map (polygon layer) and the surface temperature image of the city are superimposed and mean surface temperatures with standard deviations are computed for each land cover class by using a polygon summary Geographical Information Systems (GIS) operation. In this way, the magnitude of the surface UHI is estimated from the surface temperature differences between the different urban sites (as described by the different urban land covers) and the surrounding rural area of the city.

3. APPLICATION ON GREEK CITIES

The methodology presented above is applied to Athens (745,514 inhabitants) as well as to the major cities of Greece: Thessaloniki (363,987 inhabitants), Patra (160,400 inhabitants), Volos (82,439 inhabitants) and Heraklion (130,914 inhabitants) in order to examine their daytime thermal environment during the warm season and to also detect areas of intense thermal radiation (hot spots) within the urban settings. Finally, the daytime surface UHI intensity of each city is estimated.

Figures 1-5 illustrate the spatial distribution

of T_s values for the selected cities. Dark to bright tones indicate cooler to warmer surface temperatures. The geographical distribution of the different land covers for each city is shown in Figures 6-10. Mean surface temperatures by land cover type are shown in Table 4, whereas surface UHI intensities of the selected cities are presented in Table 5, where ΔT denotes the temperature difference in between urban-rural (*u-r*), suburban-rural (*s-r*) and mixed-rural (*m-r*) areas.

4. RESULTS AND CONCLUSIONS

It is clear from Table 4 that mixed urban areas exhibit high surface temperature values for all cities. In the case of Athens and Thessaloniki, mixed urban areas are hot spots and appear to be 3.5–4°C warmer than the surrounding rural areas, during daytime, a fact that can be attributed to intense human and industrial activities. The central area of Thessaloniki exhibits the higher surface UHI intensity (3.4°C), followed by the Patras city center (3°C). In the city of Athens, suburban and mixed urban areas are warmer than the central urban area compared to the surrounding rural. In the case of Heraklion, mixed, suburban and rural areas appear to be warmer than the central urban area of the city. In the city of Volos, urbanized areas are 1.5°C warmer than the rural areas, whereas the mixed urban areas that include industrial units are hot spots and appear to be 1.8°C warmer than the surrounding rural area.

It must be mentioned that this study was performed by using Landsat ETM+ data on individual dates of the warm season for each city. Considering that the UHI effect exhibits great spatial and temporal fluctuations and that it

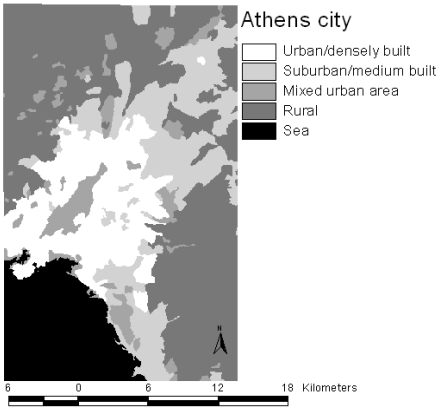

Figure 6: Land cover map of Athens ((32×20km).

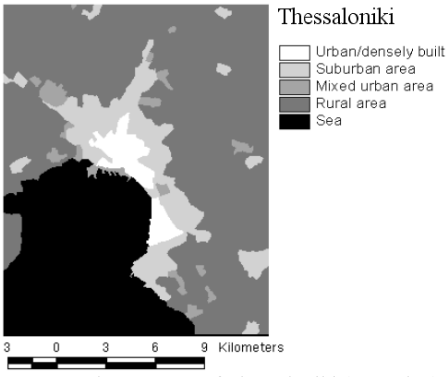

Figure 7: Land cover map of Thessaloniki (20×16km).

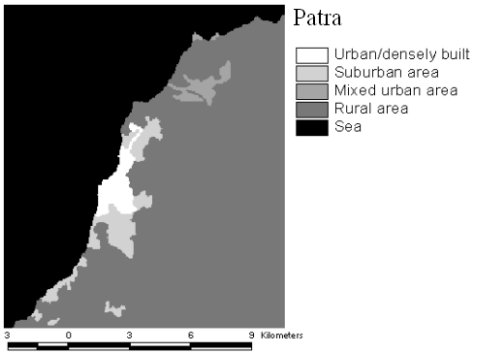

Figure 8: Land cover map of Patra (16×13km).

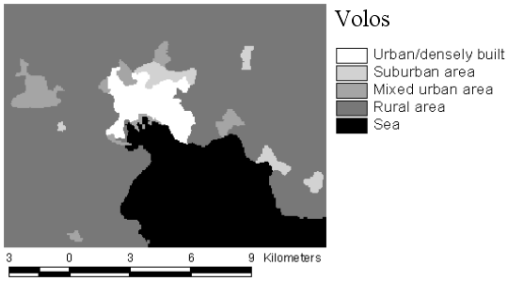

Figure 9: Land cover map of Volos (12×16km).

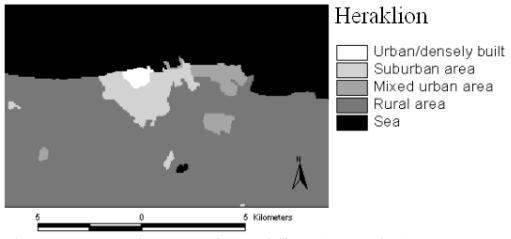

Figure 10: Land cover of Heraklion (10×15km).

Table 4: Mean values of T_s (°C) by land cover type.

City	Urban	Suburban	Mixed	Rural	Sea
Athens	30.4	32.9	33.7	30	18
Thessal.	33.4	30.8	33.4	30	23.3
Patra	33.8	32.1	30.4	30.8	20.7
Volos	36.5	35.3	36.8	35	24.4
Heraklio	39.9	42	42.5	42.8	34.6

Table 5: Estimated surface UHI intensities ΔT (in °C).

City	ΔT_{u-r}	ΔT_{s-r}	ΔT_{m-r}
Athens	0.4	2.9	3.7
Thessaloniki	3.4	0.8	3.4
Patra	3	1.3	-0.4
Volos	1.5	0.3	1.8
Heraklion	-2.9	-0.8	-0.3

strongly depends on weather conditions and synoptic flow patterns, future studies may be focused on the remote sensing UHI analysis on a monthly basis using available satellite data as well as to the development of a European consistent method for the assessment of the surface UHI effect.

REFERENCES

Aniello, C., K. Morgan, A. Busbey and L. Newland, 1995. Mapping Micro-Urban Heat Islands Using Landsat Tm and a Gis. Computers & Geosciences, 21 (8): pp. 965-969.

Dousset, B. and F. Gourmelon, 2003. Satellite multi-sensor data analysis of urban surface temperatures and landcover. Isprs Journal of Photogrammetry and Remote Sensing, 58 (1-2): pp. 43-54.

European Commission, 1994. CORINE land cover. Technical Guide. EUR 12585 EN, OPOCE, Luxembourg.

Landsat Project Science Office, 2002. Landsat 7 Science Data User's Handbook., Goddard Space Flight Center, NASA, Washington, DC.

Roth, M., T.R. Oke and W.J. Emery, 1989. Satellite-Derived Urban Heat Islands from 3 Coastal Cities and the Utilization of Such Data in Urban Climatology. International Journal of Remote Sensing, 10 (11): pp. 1699-1720.

Santamouris, M., et al., 2001. On the impact of urban climate on the energy consumption of buildings. Solar Energy, 70 (3): pp. 201-216.

Stathopoulou, M., C. Cartalis and I. Keramitsoglou, 2004. Mapping micro-urban heat islands using NOAA/AVHRR images and CORINE Land Cover: an application to coastal cities of Greece. International Journal of Remote Sensing, 25 (12): pp. 2301-2316.

Streutker, D.R., 2002. A remote sensing study of the urban heat island of Houston, Texas. International Journal of Remote Sensing, 23 (13): pp. 2595-2608.

Voogt, J.A. and T.R. Oke, 2003. Thermal remote sensing of urban climates. Remote Sensing of Environment, 86 (3): pp. 370-384.